

# The Effects of Air Temperature on Arctic Snowfall Gauge Measurements

Rachel E. Jordan,<sup>1</sup> Edgar L Andreas,<sup>2</sup> Konosuke Sugiura,<sup>3</sup> Daqing Yang<sup>4</sup>

<sup>1</sup>Jordan Environmental Modeling, PC, Hanover, NH; <sup>2</sup>NorthWest Research Associates, Inc., Lebanon, NH; <sup>3</sup>Research Institute for Global Change, Japan Agency for Marine-Earth Science and Technology, Yokosuka, Japan; <sup>4</sup>National Hydrology Research Centre, Environment Canada, Saskatoon, SK, Canada

## Measurement of Arctic snowfall is subject to large errors

Errors of 50 to 100% are not uncommon for national standard precipitation gauges in the Arctic. Low precipitation amounts make the % error larger. High winds cause lighter particles to overshoot the gauge and result in undercatchment. At speeds above 8 m s<sup>-1</sup>, snow begins to blow into the gauge and eventually leads to gauge overcatchment. Low temperatures reduce water vapor and slow the growth rate, which results in smaller particles more easily deflected by wind. Numerous studies (e.g., Yang et al. 2005) review the environmental factors detrimental to measurement accuracy in northern regions.

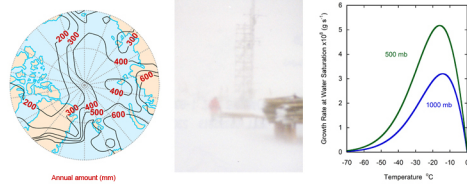


FIG. 1. Low precipitation. (After Serraz and Barry 2009) High wind/blowing snow (Photo Andreas) Low temperature/Small particle size<sup>2</sup>

## Extending measurement standards to the Arctic

The World Meteorological Organization oversaw a 7-year intercomparison program to standardize the measurement of solid precipitation in mid-latitudes. Events below 3 mm were excluded from the comparison. Snowfall in the Arctic, however, is often below this threshold; and temperatures are often 15–20°C colder than in mid-latitudes. To explore the effect of these differences on gauge catch, the Frontier Observational Research System for Global Change and the Water and Environmental Research Center, University of Alaska Fairbanks, extended the WMO intercomparison to high-latitudes with a three-year study in Barrow, Alaska.

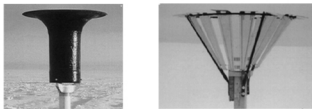


FIG. 2. Canadian Nipher and Russian Tretyakov Gauges. (Photos from Sugiura et al. 2005. © Copyright 2006 AMS)

The WMO study chose the double fence intercomparison reference (or DFIR) as a standard for “true” precipitation. The study then collected data worldwide for the DFIR and the most commonly used gauges. After correction for systematic errors, such as wetting and evaporation, the ratio of the gauge observation to the DFIR, or the “catch ratio,” was computed.<sup>3</sup> Composite data for each gauge was regressed against wind speed, the most significant factor in gauge undercatchment. Air temperature was not a significant factor, except for wet snow above -2°C.

We combine the high-latitude Barrow and the mid-latitude WMO datasets to revisit the regressions for the Canadian Nipher and Russian Tretyakov gauges. The Barrow study lowered the inclusion threshold from 3.0 mm to 0.3 mm. As a result, several snowfalls with air temperatures near -30°C are included in our analysis.

## Theoretical predictions of wind-induced undercatchment

Gauges block air flow on the windward side and accelerate flow over the top. Smaller, lighter particles track the flow more closely than do larger, denser particles. Uplift above the gauge sometimes causes them to overshoot the orifice.

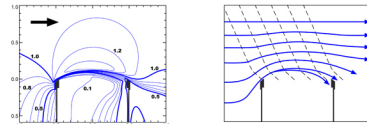


FIG. 3. MKQ gauge a) Normalized contour lines of wind flow. (After Nespor and Sevuk 1999. © Copyright 1999 AMS) b) Schematic wind and snowfall vectors.

Numerical models simulate the flow field as a function of wind speed and then compute particle trajectories within the field. Only gravity and air drag act upon the particles. Since fall velocity defines the drag coefficient, wind and fall speed determine the catch efficiency for a particular gauge.

Fall velocity ranges between ~0.5 m s<sup>-1</sup> for dendrites and 5 m s<sup>-1</sup> for graupel (Fig. 4). Dense, spherical particles have the least drag and fall fastest. For a fixed shape, velocity increases with size.

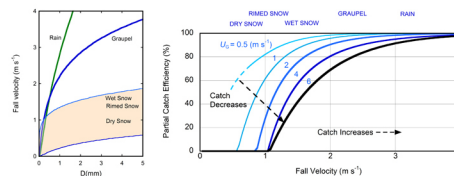


FIG. 4. Fall velocity for general categories of snow. FIG. 5. Numerical catch efficiency of raindrops as a function of fall velocity for the unshielded Hellmuth gauge.

Fig. 5 shows the variation of catch efficiency with fall velocity for selected wind speeds at gauge height ( $U_G$ ). Faster fall speeds increase the catch, while higher wind speeds reduce it. The labels across the top indicate ranges of fall velocity for general particle types. Although computed for rain drops, the curves should approximately apply to snow particles within the appropriate velocity range.

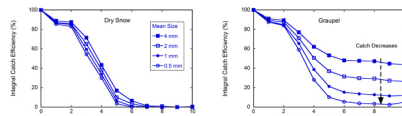


FIG. 6. Variation of the integral catch efficiency with wind speed for selected mean sizes. (After Theriault et al. 2012. © Copyright 2012 AMS)

Integrating catch efficiency with the corresponding number density and size-mass relationships yields the integral or snowfall catch efficiency and the mass-weighted fall velocity. Fig. 6 shows the computations of Theriault et al. (2012) for the shielded Alter gauge for cases of dry snow and graupel. Wind shields slow speed across the orifice and can double or triple the catch of unshielded gauges.

## Relating fall velocity to temperature

While it is possible to estimate gauge catch from wind speed and fall velocity, the wide variety of crystal habits (Fig. 7) precludes a one-to-one correspondence between fall velocity and air temperature, even if the temperature aloft is known. However, the slowing of particle growth for temperatures below ~-15°C (Fig. 1) suggests that fall velocity will, on average, decrease as well.

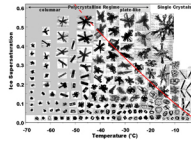


FIG. 7. Pictorial habit diagram of Bailey and Hallett (2005) based on laboratory and flight imagery. The red line indicates water saturation. (© Copyright 2009 AMS)

“Cold” and “warm” snow storm examples from the Surface Heat Budget of the Arctic Ocean experiment and the Snow Growth Model (Mitchell et al. 2006) illustrate how colder temperature affects fall velocity. The left and middle panels in Fig. 8 show millimeter-wavelength cloud radar images of Doppler velocity and radiosonde data from SHEBA. The SGM computes growth rates within the cloud using the radiosonde profiles. The right panel shows fall velocity (weighted with mass and radar reflectivity) and snowfall rate simulated with the SGM. Simulated mass fall velocities at ground level are 17% faster for the warm case, even though the assumed cloud thickness is less.

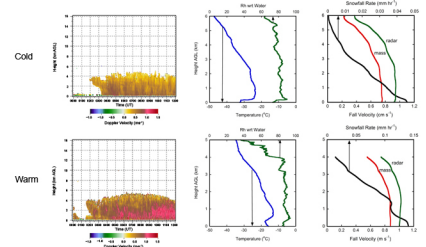


FIG. 8. Cloud imagery and data from SHEBA (left and middle panels) and the corresponding SGM simulation (right panel). We select aggregates of unrimed radiating assemblages of plates, side plates, bullets and columns (S3) as the cold crystal type (top) and the SGM “generic snow” as the warm type (bottom).

Sub-cloud evaporation occurred in many of the warmer snow events at SHEBA. This is evident in the imagery but was even more prominent in the simulations. Inclusion of riming, not yet in the SGM, would add mass and accelerate the fall velocity.

Footnotes  
<sup>1</sup> After Fig. 2.25, Serraz, M. C., and R. G. Barry, *The Arctic Climate System*, Cambridge University Press, 2005.  
<sup>2</sup> Computed from Pruppacher, H. R., and J. D. Klett, eq. 13-76, for pressure at two levels. The capacitance is 144.  
<sup>3</sup> The DFIR is first concurred with the procedure of Yang et al. (1995). For details, see Goodson, B. E., P. Y. T. Loize, and D. Yang, 1998, WMO Solid Precipitation Measurement Intercomparison, WMO/DT No. 872, IOM No. 67.  
<sup>4</sup> WMO data: source for data is as above.  
<sup>5</sup> Barrow data: Sugiura, K., T. Onishi, and D. Yang, 2006, *J. Hydrometeorol.*, 7, 984–994.  
<sup>6</sup> Nipher:  $a = -2734$ ,  $b = -0.9715$ ,  $c = 0.0782$ ,  $a_1 = -0.0613$   
<sup>7</sup> Tretyakov:  $a = -5.7436$ ,  $b = -1.0456$ ,  $c = 0.1114$ ,  $a_1 = -0.0121$   
<sup>8</sup> The SPO wind function produced corrections similar to the WMO equation but was expressed in a different form. See the website <http://www.ed.ucar.edu/projects/sheba/>; Author/Pi Moritz, R., Ice Camp Daily Precipitation Amount.

## Regression results and conclusions

Theory predicts a 100% gauge catch in calm conditions, independent of the fall velocity. In fitting the regressions, we therefore chose the following functional relationship for the catch ratio (CR):

$$CR(\%) = 100 + (aU_G + bU_G^2 + cU_G^3)(1 + a_1T_{ave}) \quad U_G \leq 12 \text{ m s}^{-1} \quad (1)$$

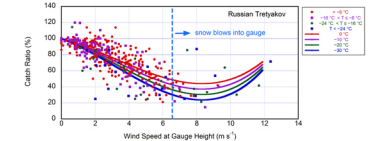
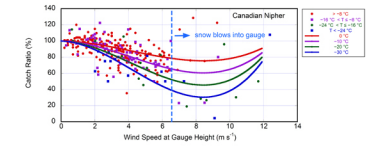


FIG. 9. Data from the combined WMO and Barrow datasets and curves computed from (1).

Using the combined WMO and Barrow data sets,<sup>4</sup> we regress CR against  $U_G$  and  $T_{ave}$  to obtain the coefficients in (1).<sup>5</sup> Fig. 9 shows the results for selected temperatures. Despite large scatter, both regressions capture the decrease in catch with falling temperatures, as predicted by theory (Fig. 5). They also show a reduction in undercatchment with the onset of blowing snow, at  $\sim U_G = 6.5 \text{ m s}^{-1}$ .

The SHEBA Project Office measured snowfall with the Nipher gauge and applied the WMO procedures to correct the data.<sup>6</sup> For ten selected storms, Matrosov et al. (2008) compared snowfall retrievals from radar at SHEBA with the SPO corrected measurements. We used eq (1) to correct the same data. Our results were generally closer to the radar retrievals and higher than the SPO values. This concurs with the assertion of Sturm et al. (2002) that the recorded measurements were biased low.

We conclude that, while there is uncertainty in predicting fall velocity from near-surface temperature, gauge catch is overall lower for cold Arctic conditions.

## Acknowledgments

The US National Science Foundation supported this work through award NSF ARC-1019322. We express our gratitude to the many WMO contributors and to the NOAA/CMDL staff and the Barrow Arctic Science Consortium for collecting the precipitation data. We thank David Mitchell for providing his Snow Growth Model, Vladislav Nespor for providing additional material on snowfall undercatchment, Janet Intieri for help with interpreting the SHEBA radar imagery, Taneli Uttal for the ETL radar velocity images, Richard Moritz for the NCAR/GLAS radiosonde data and the SPO precipitation data, and Barry Goodson for his helpful comments. We also thank Emily Moynihan of BlytheVisual, LLC, for the poster preparation.

## Contact Info

Rachel E. Jordan email: [jim.m.jordan@dartmouth.edu](mailto:jim.m.jordan@dartmouth.edu) References upon request